

THE X-RAY PROPERTIES OF $Z > 4$ QUASARS

SHAI KASPI, W. N. BRANDT, AND DONALD P. SCHNEIDER

Department of Astronomy and Astrophysics, 525 Davey Laboratory, Pennsylvania State University,
University Park, PA, 16802; shai, niel, dps@astro.psu.edu*Accepted by The Astronomical Journal*

ABSTRACT

We report on a search for X-ray emission from quasars with redshifts greater than four using the *ROSAT* public database. Our search has doubled the number of $z > 4$ quasars detected in X-rays from 6 to 12. Most of those known prior to this work were radio-loud and X-ray selected sources; our study increases the number of X-ray detected, optically selected $z > 4$ quasars from one to seven. We present their basic X-ray properties and compare these to those of lower redshift quasars. We do not find any evidence for strong broad-band spectral differences between optically selected $z > 4$ quasars and those at lower redshifts.

Subject headings: galaxies: active — galaxies: nuclei — quasars: general — X-ray: galaxies

1. INTRODUCTION

Quasars with redshifts larger than 4 were first discovered more than a decade ago (Warren et al. 1987). Recently many new $z > 4$ quasars have been discovered (e.g., Fan et al. 1999, 2000) with expectations of an even greater increase in the near future due to new surveys (e.g., the Sloan Digital Sky Survey should identify ≈ 1000 quasars with $z > 4.5$ – Schneider 1999; York et al. 2000). Currently there are 85 $z > 4$ quasars that have appeared in journals, and an additional number can be found on various World Wide Web pages. Quasars at $z > 4$ provide us with direct information about the first 10% of cosmic time. They are among the most luminous objects known, and from the Eddington limit many require $\gtrsim 10^8$ – $10^9 M_\odot$ black holes. They have wide cosmological importance since they must be associated with deep potential wells in the earliest massive collapsed structures, and their strong evolution provides clues about the process by which the remarkably homogeneous $z \approx 1000$ Universe revealed by the cosmic microwave background is transformed into the inhomogeneous Universe seen today (e.g., Efstathiou & Rees 1988; Turner 1991).

To date $z > 4$ quasars have been mainly studied at optical wavelengths (e.g., in order to determine their redshifts). There has also been some progress in studying their far-infrared and radio properties (e.g., Schmidt et al. 1995; Omont et al. 1996; McMahon et al. 1999). However, their properties as a whole at these and other wavelengths have not yet been fully explored. X-ray emission appears to be a universal property of quasars at $z \approx 0$ –2, and X-rays have also been studied from many $z \approx 2$ –4 quasars. However, at $z > 4$ the X-ray properties of quasars are much less well understood; only six $z > 4$ quasars have been detected in X-ray. The luminous X-ray emission from quasars reveals the physical conditions in the immediate vicinities of their black holes, and X-ray studies of high-redshift quasars can in principle discover if quasar central power sources and quasar environments evolve over cosmic time (e.g., Bechtold et al. 1994b; Blair et al. 1998; Elvis et al. 1998; Fiore et al. 1998).

We list the $z > 4$ quasars previously detected in the X-ray band in Table 1. For each quasar we give, in the first seven columns, its coordinates, redshift, absorption-corrected X-ray flux in the detection band, and the reference to the paper where

the X-ray detection was made. While the most basic X-ray properties (e.g., α_{ox} , the slope of a nominal power law between 2500 Å and 2 keV) of these quasars appear to be generally consistent with those of quasars at lower redshifts, the constraints are not tight and require substantial improvement. Comparisons of these properties with those of the majority of low-redshift quasars are difficult as most of the X-ray detected $z > 4$ quasars were selected in different ways: three of them are X-ray selected objects, two are radio selected, and only one is optically selected.

All objects but one in Table 1 were detected using *ROSAT*, demonstrating the ability of this satellite to detect $z > 4$ quasars. Encouraged by this we have systematically searched for detections of $z > 4$ quasars in the *ROSAT* public database. In this paper we present our results, which double the number of $z > 4$ quasars detected in X-rays. We increase the number of optically selected $z > 4$ quasars from one to seven and provide limits for 15 others. In § 2 we present the database search and in § 3 we discuss our results.

Throughout this paper we use the cosmological parameters $H_0 = 70 \text{ km s}^{-1} \text{ Mpc}^{-1}$ and $q_0 = 0.5$. We define the energy index α as $f_\nu \propto \nu^{-\alpha}$ and likewise the photon index $\Gamma = \alpha + 1$ with photon flux density $f(E) \propto E^{-\Gamma}$ in photons $\text{cm}^{-2} \text{ s}^{-1} \text{ keV}^{-1}$. Unless otherwise noted, we use $\alpha_0 = 0.5$ in the UV-optical range and $\alpha_x = 1$ in the X-ray range. These are representative values of these parameters for lower redshift quasars (e.g., Netzer 1990; Reeves et al. 1997).

2. SEARCH AND ANALYSIS

We have searched the *ROSAT* public database¹ for all fields which include the optical positions of $z > 4$ quasars in the literature. We have found 27 quasars' positions (out of the total 85 $z > 4$ quasars) to lie in *ROSAT* fields. For ten quasars we found only one observation, while for the others there were two or more. We retrieved from the *ROSAT* public database up to four observations (when available) for each quasar. We preferentially chose long observations where the quasar was close to the field's center. Twenty-six quasars were observed by the Position Sensitive Proportional Counter (PSPC; Pfeiffermann et al. 1987) with several of them also having High Resolution Imager (HRI; David et al. 1999) observations, and one quasar was ob-

¹ Via: <http://heasarc.gsfc.nasa.gov/W3Browse>

served only with the HRI. Out of the 27 quasars, 12 were the observation's target and 15 were serendipitously in the detector's field of view.

All observations were processed using the PROS software in IRAF.² We have manually inspected the images (and smoothed versions thereof) and have measured the net counts around the optical positions of the quasars. Typically PSPC positions are good to $\approx 20\text{--}30''$ (e.g., Voges et al. 1996), and indeed all our detections but one are $\lesssim 20''$ from the optical position. The aperture size for count extraction was scaled to take into account the size of the point spread function (PSF) at the off-axis angle of the quasar. We were able to detect, at above the 2.5σ level, an X-ray source and extract the X-ray count rate for nine quasars. For the other 18 quasars we were only able to determine upper limits to their X-ray count rates. We have also searched for X-ray detections of 86 quasars listed on World Wide Web pages but not in the literature, and we find none.

In the upper part of Table 2 we present the quasars detected. Their names, coordinates and redshifts are given in the first four columns. The monochromatic $AB_{1450(1+z)}$ magnitude is listed in column (5). The $AB_{1450(1+z)}$ magnitudes are from Schneider, Schmidt, & Gunn (1991), Henry et al. (1994), Storrie-Lombardi et al. (1996), and Hook & McMahon (1998), with estimated errors of $\approx \pm 0.1$ magnitudes. The Galactic column density, found using the H I map of Dickey & Lockman (1990), is given in column (6). We have used the $AB_{1450(1+z)}$ magnitude and a flux-density power law with $\alpha_0 = 0.5$ to compute the rest-frame 2500 Å flux density and luminosity which are listed in columns (7) and (8). The absolute B magnitude, given in column (9), was found using the equation

$$M_B = AB_{1450(1+z)} - 5 \log(\sqrt{1+z} - 1) - 45.03 \quad (1)$$

which is equation 5 of Schneider, Schmidt, & Gunn (1989) adapted for $H_0 = 70 \text{ km s}^{-1} \text{ Mpc}^{-1}$.

In columns (10)–(18) of Table 2 we list the X-ray observations and properties of the quasars. The sequence-ID and observing date are listed in columns (10) and (11). The angular distance of the quasar's position from the center of the field is listed in column (12). The number of background-subtracted counts (in the broad band 0.1–2 keV) is given in column (13), and the vignetting, exposure-map and background corrected count-rate is listed in column (14). We use the PIMMS software (Mukai 1997) to define a power law with photon index $\Gamma = 2$, which is then used in the XSPEC software (Arnaud 1996) to evaluate the absorption-corrected 0.1–2 keV observed flux, which is listed in column (15). From this power law we also calculated the rest-frame 2-keV flux density and luminosity which are listed in columns (16) and (17). (Using PROS to calculate these quantities yields consistent results.) Finally, we list in column (18) the effective optical-to-X-ray power-law slope, α_{ox} , defined as:

$$\alpha_{\text{ox}} = \frac{\log[(f_\nu(2 \text{ keV})/f_\nu(2500 \text{ Å}))]}{\log[\nu(2 \text{ keV})/\nu(2500 \text{ Å})]} \quad (2)$$

where f_ν 's are flux densities at the given wavelengths and ν 's are the corresponding frequencies. The uncertainties for the fluxes, luminosities, and α_{ox} values can be propagated from the relative error on the number of counts, which has a mean value of 30%. Another uncertainty involves our assumption of $\Gamma = 2$.

²IRAF (Image Reduction and Analysis Facility) is distributed by the National Optical Astronomy Observatories, which are operated by AURA, Inc., under cooperative agreement with the National Science Foundation.

Object (1)	RA (2000.0) (2)	Dec (3)	z (4)	Flux ^a (5)
Q 0000–2619	00 03 22.9	–26 03 19	4.098	$8.7 \times 10^{-14} \text{ e}$
RX J1028.6–0844	10 28 37.7	–08 44 39	4.276	8.3×10^{-13}
RX J105225.9+571905	10 52 25.9	+57 19 07	4.45	2.3×10^{-15}
GB 1428+4217	14 30 23.7	+42 04 36	4.715	$\sim 1 \times 10^{-12}$
GB 1508+5714	15 10 02.8	+57 02 44	4.301	1×10^{-12}
RX J1759.4+6638	17 59 27.9	+66 38 53	4.320	$\sim 1.2 \times 10^{-14}$

^aIn units of $\text{erg s}^{-1} \text{ cm}^{-2}$.

^bIn units of 10^{20} cm^{-2} .

^cAt 2500 Å in units of $10^{-27} \text{ ergs s}^{-1} \text{ cm}^{-2} \text{ Hz}^{-1}$.

^dAt 2 keV in units of $10^{-31} \text{ ergs s}^{-1} \text{ cm}^{-2} \text{ Hz}^{-1}$.

^eComputed using Bechtold et al. (1994a) model # 3.

^fEstimated from the 2500 Å flux given in Zickgraf et al. (1997).

REFERENCES.— (1) Bechtold et al. 1994a; (2) Zickgraf et al. 1997; (3) Schneider

As radio-quiet quasars typically have $\Gamma = 1.7\text{--}2.3$, our assumption of $\Gamma = 2$ might introduce an additional uncertainty of $\sim 15\%$ in the flux estimates. As the true Γ for each quasar is unknown (other than GB 1428+4217 and GB 1508+5714), we do not quote an error on the latter quantities. We estimate the total fractional uncertainties for the fluxes to be in the range of 30–50%.

X-ray images of all nine detected quasars are presented in Fig. 1 which was created using the adaptive smoothing method of Ebeling, White, & Rangarajan (2000) applied to the full-band images. For most of the images we used a 2.5σ level of smoothing; for three low- σ detected objects (BR 0951–0450, BRI0952–0115, and BR 1202–0725) we used a 2.0σ level of smoothing.

For each of the PSPC observations listed in the upper part of Table 2 we also calculated the X-ray counts in the soft band (0.1–0.5 keV) and the hard band (0.5–2.0 keV). We used these to calculate the rest-frame 2-keV flux density, luminosity, and α_{ox} , in the same way as described above. The results were similar to the broad-band results. However, as the statistical uncertainties in the soft and hard bands were large due the small number of counts (note the small number of counts in the broad band – column [13] of Table 2), we do not include these results in our analysis.

In the lower part of Table 2 we list the $z > 4$ quasars which we were unable to detect in the X-ray observations. For these quasars we give 3σ upper limits (listed in column [13]), where σ is the square root of the counts in an aperture of size appropriate to the quasar's off-axis angle and centered at the quasar's optical position. For each quasar we list the one observation which gave the faintest upper limit.

For 27 objects the number of expected detections which are merely statistical fluctuations at the 2.5σ level is 0.17; this suggests that none of our detections is likely to be a background fluctuation. We also estimated the probability that our X-ray quasar detections are merely of unrelated X-ray sources that happen to be coincident with the $z > 4$ quasars' optical positions. We shifted the 27 quasars' positions by eight arcmin in eight different directions and looked again for X-ray detections

TABLE 2
PROPERTIES OF QUASARS AT $z > 4$ OBSERVED BY *ROSAT*

Object (1)	RA (2000.0) (2)	Dec (3)	z (4)	AB (5)	$N_{\rm H}^{\rm a}$ (6)	$f_{\nu}^{\rm b}$ (7)	$\log(\nu L_{\nu})$ (8)	M_B (9)	Sequence-ID (10)	Date (11)	$\Delta^{\rm c}$ (12)	Counts (13)	C-rate ^d (14)	$f^{\rm e}$ (15)
Detected Quasars														
Q 0000–2619	00 03 22.9	−26 03 19	4.098	17.5	1.67	4.767	46.9	−28.0	rp700467n00	26/11/91	0.6	177±24	4.97	6.5
BR 0019–1522	00 22 08.0	−15 05 39	4.528	18.8	2.09	1.440	46.4	−26.9	rp700078n00	30/11/91	0.4	30.0±9.3	7.29	9.5
									rp701207n00	23/06/92	0.1	34±11	5.36	7.9
									rp701207a01	08/12/92	0.1	16.8±6.3	4.87	7.2
BR 0351–1034	03 53 46.9	−10 25 19	4.351	18.7 ^g	4.08	1.579	46.5	−26.9	rp700531n00	27/01/92	0.4	54±13	5.92	12.4
BR 0951–0450	09 53 55.7	−05 04 19	4.369	19.2	3.78	0.996	46.3	−26.4	rp700379n00	18/05/92	0.0	35±10	4.25	8.6
BRI0952–0115	09 55 00.1	−01 30 07	4.426	18.7	3.96	1.579	46.5	−27.0	rp700380n00	29/05/92	0.1	18.9±7.7	5.63	11.6
BR 1202–0725	12 05 23.1	−07 42 32	4.695	18.0	3.46	3.008	46.8	−27.7	rp700530n00	13/12/91	0.4	34±13	3.56	6.8
GB 1428+4217	14 30 23.7	+42 04 36	4.715	19.4	1.40	0.829	46.2	−26.4	rh704036n00	11/12/97	0.2	75±13	15.4	74.1
									rh704007n00	09/01/98	0.2	125±17	21.5	102.9
									rh704008n00	22/01/98	0.2	223±20	36.1	173.3
RX J1759.4+6638	17 59 27.9	+66 38 53	4.320	19.3	4.23	0.908	46.2	−26.3	rp000026n00	21/02/92	6.3	82±29	1.94	4.1
BR 2237–0607	22 39 53.6	−05 52 19	4.558	18.3 ^g	3.84	2.282	46.7	−27.4	rp701206n00	20/05/93	0.1	56±13	6.17	12.5
									rh800789n00	26/05/96	9.1	30±17	1.30	8.4
Undetected Quasars – X-ray Upper Limits														
PC 0027+0525	00 29 49.9	+05 42 04	4.099	21.4	3.42	0.131	45.3	−24.1	rp201077n00	09/07/92	50.1	66.2	15.13	28.9
PC 0027+0521	00 30 04.6	+05 38 13	4.210	22.3	3.43	0.057	45.0	−23.3	rp201077n00	09/07/92	49.8	80.7	18.41	35.2
Q 0046–293	00 48 29.6	−29 03 21	4.014	19.3	1.75	0.908	46.2	−26.2	rp700275n00	01/06/92	47.2	134.0	10.00	13.4
Q 0051–279	00 54 15.4	−27 42 08	4.395	19.2	1.72	0.996	46.3	−26.4	rp701223n00	03/07/92	43.1	133.8	4.38	5.8
Q 0101–304	01 03 37.3	−30 08 59	4.072	20.0	2.03	0.477	45.9	−25.5	rp701194n00	06/07/92	0.4	18.5	1.38	2.0
BRI0103+0032	01 06 19.2	+00 48 23	4.433	18.8	3.19	1.440	46.4	−26.7	rh703871n00	22/12/97	17.1	111.4	8.89	54.2
SDSS033829.31+002156.3	03 38 29.3	+00 21 56	5.000	20.0	8.11	0.477	46.0	−25.8	rp200844n00	26/01/92	28.5	26.2	12.70	35.6
PC 0953+4749 ^h	09 56 25.2	+47 34 44	4.457	19.1	0.98	1.092	46.3	−26.6	rp700450n00	12/05/92	13.5	21.4	6.53	6.6
RX J105225.9+571905 ⁱ	10 52 25.9	+57 19 07	4.450	22.6	0.56	0.043	44.9	−23.1	rp900029a00	16/04/91	4.0	60.5	0.97	0.8
BRI 1050–0000	10 53 20.4	−00 16 49	4.291	19.4	3.95	0.828	46.2	−26.2	rp700381n00	26/05/92	0.4	18.2	4.00	8.2
BR 1144–0723	11 46 35.6	−07 40 05	4.147	18.8	3.75	1.440	46.4	−26.7	rp700382n00	05/06/92	0.3	13.4	2.94	5.9
SDSS122600.68+005923.6	12 26 00.7	+00 59 24	4.250	19.1	1.89	1.092	46.3	−26.5	rp600242a01	24/12/92	44.7	131.6	12.61	17.6
PC 1233+4752	12 35 31.1	+47 36 06	4.447	20.1	1.18	0.435	45.9	−25.6	rp200578n00	14/11/91	22.8	33.7	21.07	23.1
PKS 1251–407	12 53 59.5	−40 59 31	4.458	19.6 ^j	7.97	0.689	46.1	−26.1	rp800321a01	18/01/93	36.4	59.6	9.27	25.8
SDSS131052.52–005533.4	13 10 52.5	−00 55 33	4.140	18.9	1.77	1.313	46.3	−26.6	rp800248n00	18/07/92	26.8	49.6	6.51	8.8
Q 2133–4311	21 36 23.7	−42 58 18	4.200	20.9 ^{g,k}	2.84	0.208	45.6	−24.7	rp800336a01	06/05/93	30.8	43.6	5.35	9.3
Q 2139–4324	21 42 58.2	−43 10 59	4.460	20.7 ^{g,k}	2.45	0.250	45.7	−25.0	rp300274n00	28/04/93	29.7	65.3	11.69	18.7
PC 2331+0216	23 34 31.9	+02 33 22	4.093	19.8	4.81	0.573	46.0	−25.7	rh701901n00	24/12/94	0.2	30.1	1.93	13.4

^aIn units of 10^{20} cm^{-2} .^bAt 2500 Å in units of $10^{-27} \text{ ergs s}^{-1} \text{ cm}^{-2} \text{ Hz}^{-1}$.^cOffset from the field center in units of arcmin.^dIn units of $10^{-3} \text{ counts s}^{-1}$.^eFlux at the 0.1–2 keV band in units of $10^{-14} \text{ ergs s}^{-1} \text{ cm}^{-2}$.^fAt 2 keV in units of $10^{-31} \text{ ergs s}^{-1} \text{ cm}^{-2} \text{ Hz}^{-1}$.^gEstimated using an empirical linear relation between $[APM R - AB_{1450(1+z)}]$ and $[z]$ for all objects in Storrie-Lombardi (1996) and deriving the missing $AB_{1450(1+z)}$ from that relation.^hFor better upper-limit determination see Molthagen, Wendker, & Briel (1995).ⁱCan be only detected by careful co-adding of many observations (see Table 1 and Schneider et al. 1998).^jFrom Shaver et al. (1996); using the m_i magnitude to estimate AB and the 1.4 GHz flux density to estimate R .^kEstimated using m_R magnitudes from and Hawkins & Véron (1996).

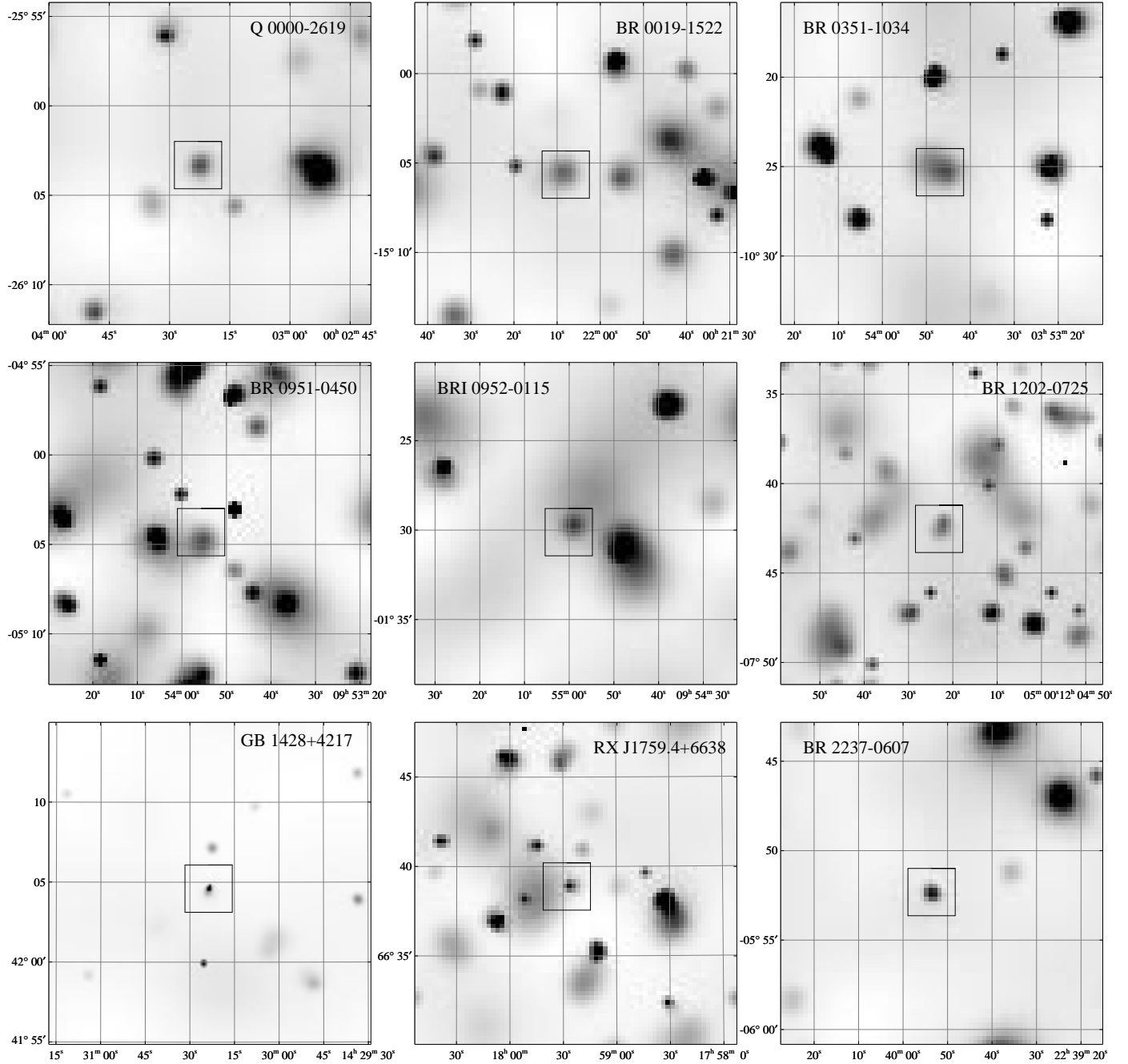


FIG. 1.— *ROSAT* images of the nine detected $z > 4$ quasars from 0.1–2.4 keV. North is up and East is to the left. The horizontal axis shows the Right-Ascension, and the vertical axis shows the Declination in J2000 coordinates. The box in each image is centered on the optical coordinates of the quasar, and its size is substantially larger than the positions uncertainty. Each image is $\approx 18' \times 18'$. All images are from the PSPC except for GB 1428+4217 which is from the HRI.

(in the same manner as was done for the real optical positions). At the new positions we found seven X-ray sources which met our detection criteria regarding significant level and positional coincidence. This test shows that among our nine X-ray detections there might be one source which is not the counterpart of the quasar but an X-ray source which happened to be in that position by chance. Additional suggestive evidence that the number of false detections is small is that we have detected only the brighter quasars out of the total 27 (see Fig. 2 and § 3); if our detections had random contamination by foreground sources then their distribution would not be correlated with quasar luminosity.

For comparison purposes we present some properties of the X-ray detected $z > 4$ quasars known prior to this work in Table 1. We list the $AB_{1450(1+z)}$ magnitudes in column (8) and the Galactic column densities in column (9). Based on the $AB_{1450(1+z)}$ magnitudes we calculate the rest-frame 2500 Å flux densities and luminosities which are listed in columns (10) and (11), and the absolute B magnitudes in column (12). We used the X-ray fluxes and bands from columns (5) and (6) and the PIMMS software to define a simple power law with $\Gamma = 2$. This power law was used to estimate the rest-frame 2-keV flux den-

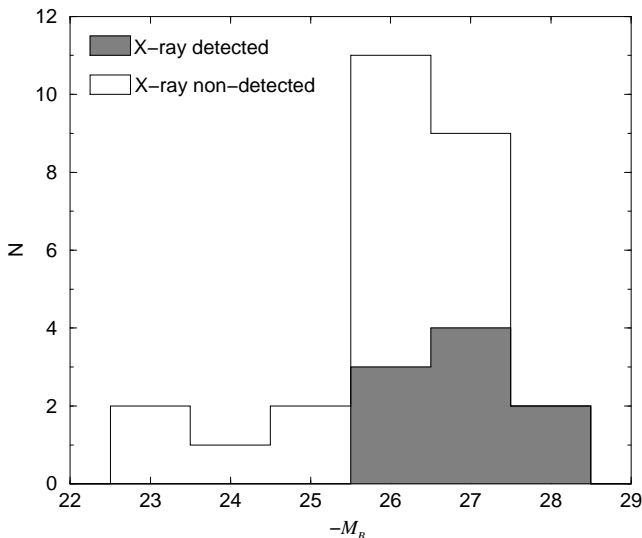


FIG. 2.— M_B distribution of the 27 $z > 4$ quasars observed by *ROSAT*. The shaded area represents the quasars which were X-ray detected.

sity and luminosity which are listed in columns (13) and (14). We list the resulting α_{OX} in column (15).

3. DISCUSSION

In most cases where we detect X-ray sources at the quasars' optical positions they are very close to the detection limit. Comparing the data for the quasars which are X-ray detected to those which are not, we notice several trends. The detected quasars are among the brighter in the optical band (see Fig. 2 for the M_B distribution). If the undetected quasars have comparable X-ray luminosities to the detected ones, we suggest that they were mainly not detected since they were observed at the edges of the PSPC field where the PSF and vignetting are larger. In the two cases where high luminosity quasars were observed close to the PSPC field center (BRI 1050–0000, BR 1144–0723), we

attribute the non-detections to short exposure times.

Three objects which we detected had already been reported as X-ray emitters in the past (Q 0000–2619, GB 1428+4217, and RX J1759.4+6638). The X-ray properties we have measured for them are in agreement with the previous reported properties (see Table 1). We have not detected the other three quasars in Table 1 since the data for RX J1028.6–0844 are not public (it was detected in the *ROSAT* All-Sky Survey), GB 1508+5714 was not observed by *ROSAT*, and RX J105225.9+571905 could be detected only in the “ultra-deep” HRI survey (see Schneider et al. 1998 and references therein).

At present only a few radio-loud $z > 4$ quasars are known. These include GB 1428+4217, GB 1508+5714, and RX J1028.6–0844 which have had their X-ray data published prior to this work (Table 1), PKS 1251–407, for which we present an X-ray upper limit, and GB 1713+2148, whose *ROSAT* observation is not yet public. Out of these objects, GB 1428+4217 and GB 1508+5714 show evidence for relativistic beaming (e.g., Moran & Helfand 1997; Fabian et al. 1999). We used the NRAO³ VLA Sky Survey (NVSS; Condon et al. 1998) catalog and images at 1.4 GHz to estimate the quasars' radio loudnesses, R , defined as the ratio of the radio flux (extra-

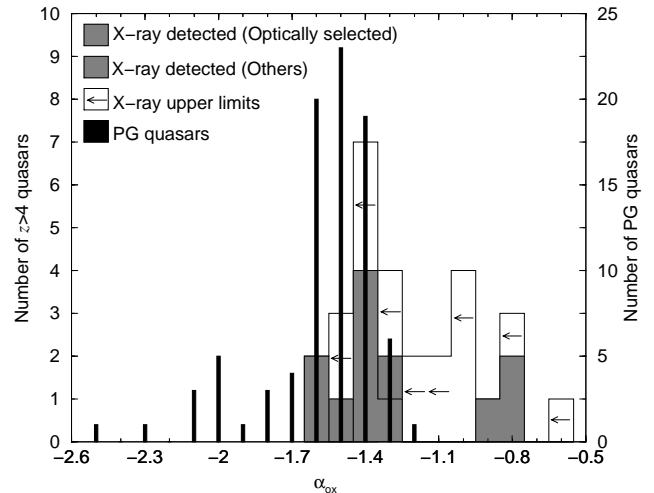


FIG. 3.— α_{OX} distribution of X-ray detected $z > 4$ quasars (shaded areas) compared with the α_{OX} distribution of the 87 $z < 0.5$ PG quasars (black bars) from Brandt et al. (2000; including four upper limits). We distinguish between $z > 4$ quasars which are optically selected and those which are selected from X-ray and radio samples. The distribution of $z > 4$ X-ray upper-limits is also shown (white bars with arrows).

cted from the NVSS) to the optical flux at 4400 Å (estimated using the AB magnitude and a flux-density power law with $\alpha_o = 0.5$). Radio-loud quasars typically have $R > 100$ and radio-quiet quasars have $R < 10$ (e.g., Kellermann et al. 1989). We list R in Table 1 column (16) and Table 2 column (19). Most of the quasars in this study are undetected by the NVSS, and thus we provide only upper limits⁴. In addition to the above mentioned radio-loud quasars we detect PC 0027+0525 to be radio-loud and BRI 1050–0000, RX J1759.4+6638, and PC 2331+0216 to be intermediate between the two radio classes (see also McMahon et al. 1994). All other quasars (but two) have R upper limits which designate them as being radio-quiet.

³The National Radio Astronomy Observatory is a facility of the National Science Foundation operated under cooperative agreement by Associated Universities, Inc.

⁴The results reported here from the NVSS are consistent with those from the Faint Images of the Radio Sky at Twenty-cm (FIRST; Becker, White, & Helfand 1995) which currently covers only a third of our objects.

This result is in agreement with other radio and far-IR studies of these $z > 4$ quasars which find them to be radio-quiet (e.g., Schneider et al. 1992; Omont et al. 1996; McMahon et al. 1999). Our results are also consistent with the Schmidt et al. (1995) conclusion that only 5–10% of optically selected $z > 4$ quasars are radio-loud.

In Fig. 3 we compare the α_{OX} distribution of all the X-ray detected $z > 4$ quasars with the α_{OX} distribution of a sample of all 87 Palomar-Green (PG) quasars at $z < 0.5$ from Brandt, Laor, & Wills (2000). We have translated the α_{OX} given in Brandt et al. (2000) for a flux density at 3000 Å to that for a flux density at 2500 Å. To carry out this comparison we consider only the optically selected $z > 4$ quasars⁵ since the PG sample is an optically selected sample. The α_{OX} distribution for the seven optically-selected objects is consistent with the α_{OX} distribution of the PG quasars and with the α_{OX} distribution usually found for quasars (e.g., Wilkes et al. 1994; Green et al. 1995). We also use all optically selected objects in this study, including the ones with upper limits on their X-ray properties, to derive the mean α_{OX} . To that purpose we have used the ASURV software package Rev 1.2 (LaValley, Isobe & Feigelson 1992), which implements the survival analysis methods presented in Feigelson & Nelson (1985) and Isobe, Feigelson, & Nelson (1986).

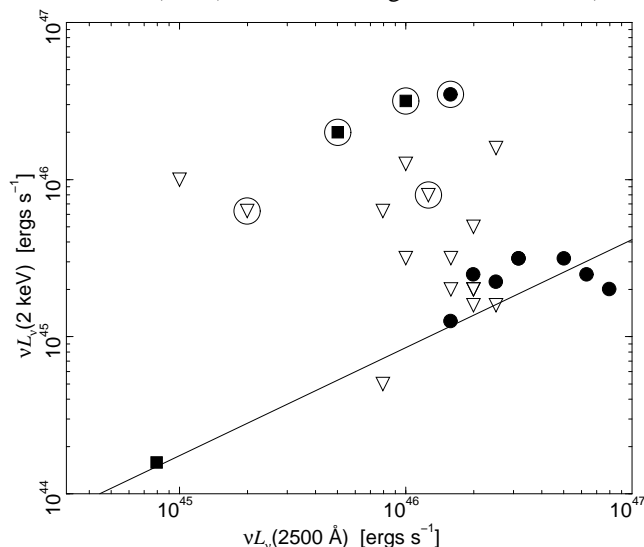


FIG. 4.— Rest-frame 2 keV versus 2500 Å luminosities. Filled circles are data from this study, squares are data from previous studies, and empty triangles are upper limits determined in this study. Radio-loud quasars are circled. The separation between the three blazar-type (highest points) from the other objects is clearly visible.

We find the mean α_{OX} to be -1.49 ± 0.04 which is in agreement with past studies.

Three of the detected quasars have $\alpha_{\text{OX}} < -1$ (Fig. 3). This is not consistent with the PG quasars' α_{OX} distribution, and indeed these three quasars are the ones known to be radio-loud with two of them being blazar-type objects, while the PG quasars

are mainly radio-quiet with no blazars among them.

The separation between the blazar-type and radio-quiet quasars can also be seen in Fig. 4, where we plot the rest-frame 2 keV versus 2500 Å luminosities. The X-ray fluxes for the three radio-loud quasars are about an order of magnitude higher than those of the radio-quiet ones. A line fit to the radio-quiet quasars' data using ASURV yields

$$\frac{\nu L_{\nu}(2 \text{ keV})}{10^{45} \text{ ergs s}^{-1}} = (0.175^{+0.070}_{-0.050}) \left[\frac{\nu L_{\nu}(2500 \text{ Å})}{10^{45} \text{ ergs s}^{-1}} \right]^{0.69 \pm 0.10} \quad (3)$$

This relation is in agreement with the one found for lower-redshift quasars (e.g., Wilkes et al. 1994; Green et al. 1995), albeit within relatively large uncertainty owing to the small number of points and their distribution.

Three of our detected quasars have two *ROSAT* observations (Table 2). In all cases the fluxes from different observations agree to within the measurement uncertainty of $\sim 30\%$, and no flux variations over time are detected. The quasar GB 1428+4217 has six *ROSAT* observations and was found to vary by a factor of two over a timescale of two weeks (or less), which corresponds to less than 2.5 days in the source's rest-frame, a result not unexpected in that this quasar is a flat-spectrum radio-loud blazar (Fabian et al. 1998, 1999).

The observed 0.1–2 keV band corresponds to a rest-frame band of 0.5–10 keV at $z = 4$. Emission at the low end of this bandpass can originate from an accretion disk, but is mainly thought to arise from the surrounding corona (e.g., Fabian 1994). Detecting X-ray emission in this band from $z > 4$ quasars suggests that similar processes are taking place in low-redshift and the highest-redshift quasars.

We have established that in almost all cases where $z > 4$ quasars were observed at the center of the PSPC field and the exposure times were sufficiently long (as anticipated from their optical luminosities), an X-ray source was found at the optical position of the quasar. As two, and possibly three, of the objects detected before our paper are “peculiar” blazar-type objects, we have more than doubled the number of optically selected $z > 4$ quasars detected in the X-ray band and determined that α_{OX} in these quasars is similar to that of lower z quasars. At present we have only been able to study in X-rays the most luminous $z > 4$ quasars. New X-ray missions such as *Chandra*, *XMM*, *Constellation-X*, and *XEUS* should allow the study of the X-ray properties of considerably less luminous $z > 4$ quasars. With thousands of $z > 4$ quasars expected to be found in the next few years (e.g., by the Sloan Digital Sky Survey), there should be ample targets.

We are grateful for several valuable suggestions by David J. Helfand. We acknowledge the support of NASA LTSA grant NAG5-8107 (SK, WNB), the Alfred P. Sloan Foundation (WNB), and NSF grant 99-00703 (DPS). We thank Harald Ebeling for the use of his IDL software.

REFERENCES

- Arnaud, K. A. 1996, in *Astronomical Data Analysis Software and Systems*, ASP Conference Series 101, ed. G. Jacoby, & J. Barnes, (San Francisco: ASP), 17
- Bechtold, J., et al. 1994a, *AJ*, 108, 374
- Bechtold, J., et al. 1994b, *AJ*, 108, 759
- Becker, R. H., White, R. L., & Helfand, D. J. 1995, *AJ*, 450, 559
- Blair, A. J., Stewart, G. C., Georgantopoulos, I., Boyle, B. J., Almaini, O., Shanks, T., Gunn, K. F., & Griffiths, R. E. 1998, *Astr. Nach.*, 319, 25
- Brandt, W. N., Laor, A., & Wills, B. J. 2000, *ApJ*, in press (astro-ph/9908016)
- Condon, J. J., Cotton, W. D., Greisen, E. W., Yin, Q. F., Perley, R. A., Taylor, G. B., & Broderick, J. J. 1998, *AJ*, 115, 1693

⁵The only objects which are not optically selected in our study are the five last objects listed in Table 1.

- David, L. P., Harnden, F. R., Kearns, K. E., & Zombeck, M. V. 1999, The *ROSAT* High Resolution Imager Calibration Report. U.S. *ROSAT* Science Data Center, Cambridge
- Dickey, J. M., & Lockman, F. J. 1990, *ARA&A*, 28, 215
- Ebeling, H., White, D. A., & Rangarajan, F. V. N. 2000, *MNRAS*, submitted
- Efstathiou G., & Rees M. J. 1988, *MNRAS*, 230, L5
- Elvis, M., Fiore, F., Giommi P., & Padovani P. 1998, *ApJ*, 492, 91
- Fabian, A.C. 1994, *ApJS*, 92, 555
- Fabian, A. C., Brandt, W. N., McMahon, R. G., & Hook, I. M. 1997, *MNRAS*, 291, L5
- Fabian, A. C., Iwasawa, K., Celotti, A., Brandt, W. N., McMahon, R. G., & Hook, I. M. 1998, *MNRAS*, 295, L25
- Fabian, A. C., Celotti, A., Pooley, G., Iwasawa, K., Brandt, W. N., McMahon, R. G., & Hoenig, M. D. 1999, *MNRAS*, 1999, 308, L6
- Fan, X., et al. 1999, *AJ*, 118, 1
- Fan, X., et al. 2000, *AJ*, 119, in press
- Feigelson, E. D., & Nelson, P. I. 1985, *AJ*, 293, 192
- Fiore, F., Elvis, M., Giommi, P., & Padovani, P. 1998, *ApJ*, 492, 79
- Green, P. J., et al. 1995, *ApJ*, 450, 51
- Hawkins, M. R. S., & Véron, P. 1996, *MNRAS*, 281, 348
- Henry, J. P., et al. 1994, *AJ*, 107, 1270
- Hook, I. M., & McMahon, R. G. 1998, *MNRAS*, 294, L7
- Isobe, T., Feigelson, E. D., & Nelson P. I. 1986, *AJ*, 306, 490
- Kellermann, K. I., Sramek, R., Schmidt, M., Shaffer D. B., Green, R. F. 1989, *AJ*, 98, 1195
- LaValley, M., Isobe, T., & Feigelson, E. D. 1992, in *Astronomical Data Analysis Software and Systems*, ASP conference series 25, ed. D. M. Worrall, C. Biemesderfer, & J. Barnes, (San Francisco: ASP), 245
- Mathur, S., & Elvis, M. 1995, *AJ*, 110, 1551
- McMahon, R. G., Omont, A., Bergeron, J., Kreysa, E., Haslam, C. G. T. 1994, *MNRAS*, 267, L9
- McMahon, R. G., Priddey, S. R., Omont, A., Snellen, I., & Withington, S. 1999, *MNRAS*, 309, L1
- Molthagen, K., Wendker, H. J., & Briel, U. G. 1995, *A&A*, 295, 43
- Moran, E. C., & Helfand, D. J. 1997, *ApJ*, 484, L95
- Moran, E. C., Helfand, D. J., Becker, R. H., & White, R. L. 1996, *ApJ*, 461, 127
- Mukai, K. 1997, The PIMMS Users' Guide (Greenbelt: NASA/GSFC)
- Netzer, H. 1990, in *Active Galactic Nuclei*, ed., T. J. -L. Courvoisier, & M. Mayor (Berlin: Springer-Verlag), 57
- Omont, A., McMahon, R. G., Cox, P., Kreysa, E., Bergeron, J., Pajot, F., & Storrie-Lombardi, L. J. 1996, *A&A*, 315, 1
- Pfeffermann, E., et al., 1987, *Proc. SPIE*, 733, 519
- Reeves, J. N., Turner, M. J. L., Ohashi, T., & Kii, T. 1997, *MNRAS*, 292, 468
- Schmidt M., van Gorkom J. G., Schneider D. P., Gunn J. E. 1995, *AJ*, 109, 473
- Schneider, D. P. 1999, in *After the Dark Ages: When Galaxies were Young*, ed. S. Holt, & E. Smith, (American Institute of Physics Press), 233
- Schneider, D. P., Schmidt, M., & Gunn J. E. 1989, *AJ*, 98, 1507
- Schneider, D. P., Schmidt, M., & Gunn J. E. 1991, *AJ*, 101, 2004
- Schneider, D. P., van Gorkom, J. H., Schmidt, M., & Gunn, J. E. 1992, *AJ*, 103, 1451
- Schneider, D. P., Schmidt, M., Hasinger, G., Lehmann, I., Gunn, J. E., Giacconi, R., Trümper, J., & Zamorani, G. 1998, *AJ*, 115, 1230
- Shaver, P. A., Wall, J. V., & Kellermann, K. I. 1996, *MNRAS*, 278, L11
- Storrie-Lombardi, L. J., McMahon, R. G., Irwin, M. J., & Hazard, C. 1996, *ApJ*, 468, 121
- Turner, E. L. 1991, *AJ*, 101, 5
- Voges, W., et al. 1996, in *Röntgenstrahlung from the Universe*, ed. H. U. Zimmermann, J. Trümper, & H. Yorke, MPE Report 263, 637
- Warren, S. J., Hewett, P. C., Irwin, M. J., McMahon, R. G., & Bridgeland, M. T. 1987, *Nature*, 325, 131
- Wilkes, B. J., Tananbaum, H., Worrall, D. M., Avni, Y., Oey, M. S., & Flanagan, J. 1994, *ApJS*, 92, 53
- York, D. G., et al. 2000, *AJ*, submitted
- Zickgraf, F. -J., Voges, W., Krautter, J., Thiering, I., Appenzeller, I., Mujica, R., & Serrano, A. 1997, *A&A*, 323, L21

